Alexandria Engineering Journal (2016) 55, 2023–2033

HOSTED BY

ELSEVIER

Alexandria University

Alexandria Engineering Journal

www.elsevier.com/locate/aej
www.sciencedirect.com

ORIGINAL ARTICLE

Effect of heat transfer on unsteady MHD flow of blood in a permeable vessel in the presence of non-uniform heat source

A. Sinha [a,*], J.C. Misra [b], G.C. Shit [a]

[a] Department of Mathematics, Jadavpur University, Jadavpur 700032, India
[b] Indian Institute of Technology, Kharagpur, India

Received 17 June 2015; revised 8 July 2016; accepted 11 July 2016
Available online 24 August 2016

KEYWORDS

Permeable capillary;
Unsteady stretching motion;
Non-uniform heat source/sink;
Velocity-slip;
Temperature-jump

Abstract This paper presents a theoretical analysis of blood flow and heat transfer in a permeable vessel in the presence of an external magnetic field. The unsteadiness in the coupled flow and temperature fields is considered to be caused due to the time-dependent stretching velocity and the surface temperature of the vessel. The non-uniform heat source/sink effect on blood flow and heat transfer is taken into account. This study is of potential value in the clinical treatment of cardiovascular disorders accompanied by accelerated circulation. The problem is treated mathematically by reducing it to a system of coupled nonlinear differential equations, which have been solved by using similarity transformation and boundary layer approximation. The resulting nonlinear coupled ordinary differential equations are solved numerically by using an implicit finite difference scheme. Computational results are obtained for the velocity, temperature, the skin-friction coefficient and the rate of heat transfer in the vessel. The estimated results are compared with another analytical study reported earlier in scientific literatures. The present study reveals that the heat transfer rate is enhanced as the value of the unsteadiness parameter increases, but it reduces as the space-dependence parameter for heat source/sink increases.

1. Introduction

Although heat transfer is primarily an important domain of Thermal Engineering, attempts have been successfully made by several researchers to apply its principles to explore a variety of information on how the body transfers heat [1]. Several mathematical models have also been developed, which have been applied to cryopreservation, as well as cryosurgery and laser surgery. These models have also found useful applications in various modern techniques of physiotherapy, that involve heating the affected portion of the human body. Moreover, as discussed in our previous communication [2], the therapeutic procedure of electromagnetic hyperthermia, where the cancerous tissues are exposed to a thermal environment of 42 °C, while maintaining the surrounding normal tissues at a suitable temperature, formulation and analysis of

* Corresponding author.
E-mail address: aniruddha.sinha07@gmail.com (A. Sinha).
Peer review under responsibility of Faculty of Engineering, Alexandria University.

http://dx.doi.org/10.1016/j.aej.2016.07.010

Nomenclature

η	dimensionless distance
u	velocity of blood along the axis of the capillary
v	transverse velocity of blood in the capillary
T	temperature of blood at any point within the capillary
u_s	velocity-slip at the wall
U_w	stretching velocity
V_w	injection/suction velocity
T_w	surface temperature
T_s	thermal slip
T_0	a constant denoting the reference temperature
g	acceleration due to gravity
$B(t)$	time-dependent magnetic field intensity
q'''	non-uniform heat generation/absorption
$k_1(t)$	time-dependent permeability parameter of blood
k_2	constant permeability of the medium
k_3	non-dimensional permeability parameter
k	thermal conductivity of blood
N	velocity-slip factor
K	thermal slip factor
M	Hartmann number of the blood mass
S	unsteadiness parameter
λ	buoyancy parameter
S_f	non-dimensional velocity-slip factor
S_t	non-dimensional thermal slip factor
Pr	Prandtl number
A	injection/suction parameter
ρ	density of blood
σ	electrical conductivity of blood
ν	coefficient of kinematic viscosity of blood
β	coefficient of thermal expansion
c_p	specific heat at constant pressure
$A^\star$	space-dependent heat generation/absorption
$B^\star$	temperature-dependent heat generation/absorption
C_f	skin-friction coefficient
Nu_x	local Nusselt number

mathematical models on heat transfer during blood flow have been found to be very useful.

In the human circulatory system, blood flowing through different branches of the arterial/venous tree, heat is distributed through tissues evenly to the whole body and so heat cannot accumulate in any part of the tissue medium. The different components for calculating the total quantity of heat that blood carries when it flows through blood vessels include blood velocity, vessel diameter, thickness of blood, temperature of the surrounding tissues and heat transfer coefficient of blood. But since the first three factors are included in Reynolds number, one can quantify the heat carried by blood only through the consideration of temperature of the tissues, together with the heat transfer coefficient of blood and the Reynolds number.

Measurement of blood flow rate is of great interest to clinicians, medical scientists and biomedical engineers. It is very useful in the diagnosis of various arterial/venous diseases, e.g., atherosclerosis, atheroma. These diseases deter the normal flow of blood.

Variation in blood flow due to changes in the temperature was investigated by Barcroft and Edholm [3]. Barozzi and Dumas [4] used a numerical method to study the convective heat transfer in blood vessels of the circulatory system. They observed that the rheological behavior of blood does not significantly affect the heat transfer rate in small blood vessels. It is to be noted that the main source of heat produced in the human body is the process of metabolism of nutrients that takes place in a ceaseless manner. This supplies energy to the various organs of the body. It has been reported in the scientific literatures that in a human body at rest, about two-thirds of the total heat is generated by the metabolic activities of the internal organs in the thorax, the abdomen and the brain; the share of the heat generated in the brain being around 16% of the total heat generated in the whole body. However, in order that the human body can function properly, the internal temperature of the body must always remain consistent. For this purpose, it is necessary that if any excess heat is generated in the body due to any reason, it must have to be dissipated out of the body as early as possible. The manner in which the transfer of heat in the living human body takes place is somewhat complicated, owing to the fact here it is a combination of thermal conduction, convection and metabolic heat production. Conduction (also called diffusion) takes place in tissues, while convection occurs in the case of blood and other body fluids.

Convective heat transfer during blood flow in small tubes was studied analytically by Wang [5] in the case of fully developed flow with constant heat flux.

Pennes [6] formulated a simplified bio-heat transfer model in order to illustrate the effects of blood perfusion and metabolic heat generation in living tissues. Although this model bears the potential to describe the effect of blood flow on tissue temperature, it has some serious shortcomings, because he assumed uniform perfusion rate and did not account for the direction of blood flow. Moreover, in his model he considered only the stream of venous blood as the fluid stream equilibrated with tissue. Subsequently, several other models were proposed by other researchers, in which some of the shortcomings were removed. Nakayama and Kuwahara [7] presented a mathematical analysis of the bio-heat transfer problem by using volume averaging theory. Some of the shortcomings of Pennes model [6] could be removed in this study. Keeping in view that large blood vessels can produce steep temperature gradients in heated tissues leading to inadequate tissue temperatures during hyperthermia, Colios et al. [8] used numerical techniques to solve a problem concerning the cooling of large blood vessels in a heated tissue medium. Chato [9] investigated heat transfer to individual blood vessels in three different configurations: a single vessel, two vessels in counter flow, and a single vessel near the skin surface. Heat transfer in perfused tissues in the presence of a vessel was studied by Rai and Rai [10],

considering metabolic heat generation and blood perfusion in the tissue as temperature-dependent.

Nilsson [11] made an attempt to determine the relationship between skin blood flow and temperature. Another study on the relationship between blood circulation and peripheral temperature was conducted both experimentally and numerically by He et al. [12]. He et al. [13] reported another study of thermo-fluid model of blood circulation. In this study, the influence of bending stiffness of the vessel and that of blood viscosity on blood pressure and temperature were analyzed. The heat convection coefficient in large blood vessels was evaluated mathematically by Consiglieri et al. [14] to show that heating a large portion of blood vessel reduces convective heat loss. A physiology-based algorithm for simulating of a realistic vascular tree containing all thermally significant vessels in a tissue medium was suggested by Baish [15]. Some experimental investigations on the role of blood as heat source/sink in human organs and temperature variation along artery-vein pairs were carried out respectively by Ducharme and Tikuisis [16] and He et al. [17]. Srinivas et al. [18] theoretically studied an unsteady hydromagnetic heat and mass transfer of blood in a time-dependent porous blood vessel over a permeable stretching sheet in the presence of thermal radiation, chemical reaction and slip conditions.

In the recent years, the study of magnetohydrodynamic (MHD) flow of blood through arteries has gained considerable interest because of its important applications in physiology. It is known that blood is a suspension of various cells in plasma, the main bulk of the cells being erythrocytes. Since erythrocytes have negative charge (although small), an applied magnetic field can influence the motion of erythrocytes; thus, blood flow is affected due to the action of an external magnetic field. The potential use of the magnetohydrodynamic principles in the prevention and rational therapy of the arterial hypertension was explored by Vardanyan [19], who found that for steady flow of blood in an artery of circular cross section, a uniform transverse magnetic field alters the flow rate of blood. Sud and Sekhon [20] numerically studied the effect of magnetic field on blood flow though the human arterial system. Haldar and Ghosh [21] investigated the effect of magnetic field on blood flow through an indented tube in the presence of erythrocytes. According to the investigation reported by Barnothy [22], the heat rate decreases when a biological system is exposed to an external magnetic field. The electrocardiographic (ECG) pattern taken in the presence of a magnetic field can not only provide information on blood flow, but also offers a new non-invasive method for studying the cardiac performance. A three-parameter rheological model was used by Kirkovskii et al. [23] in order to study the influence of a variable magnetic field on the rheological properties of blood of patients suffering from rheumatoid arthritis. The parameters of the model are related to hydrodynamic properties of erythrocytes suspension. They observed that out of the three parameters considered in their study, only one has the capacity to alter the rheological properties of blood to an appreciable extent.

The major activity of the entire cardiovascular system is to supply blood to tissues under sufficient pressure gradient to exchange materials through arterial wall. Small arteries are thin-walled and consist of endothelial cells. They contain ultra-microscopic pores through which substances of various molecular sizes can penetrate inside and pass into the lumen of the arteries from the surrounding tissues. Although pulsatile flow through permeable walls is important in understanding blood flow in the entire circulatory system, not much work has been done in this direction.

Oka and Murata [24] made a theoretical study on the steady motion of blood through a permeable vessel obeying Starling's law. Mariamma and Majhi [25] analyzed the steady laminar flow of blood as a single phase of homogeneous Newtonian fluid in tubes with permeable walls. A discussion relevant to the boundary conditions between a porous medium and a viscous fluid was made by Beavers and Joseph [26]. Their analysis and experiment were, however focused on a rectangular channel with a porous wall in which fluid flows under the action of a pressure gradient. Saffman [27] developed a generalized Darcy equation for non-uniform flows in non-homogeneous porous media. The boundaries were considered as discontinuous changes of properties of the porous media.

The flow over a stretching surface has received attention of several researchers in the past. Misra and Shit [28,29] developed mathematical models for investigating the flow of a viscoelastic fluid over a stretching sheet as well as in a channel with stretching walls under the action of an externally applied magnetic field generated by a magnetic dipole. Misra et al. [30] also investigated the flow and heat transfer of an MHD viscoelastic fluid in a channel with stretching walls.

It is known that a viscous fluid normally sticks to a boundary, i.e., there is no slip of the fluid relative to the boundary. Misra et al. [31] conducted a study concerning blood flow through a stenosed arterial segment, considering no-slip condition at the vessel wall. For many fluids, such as particulate fluids, the motion is still governed by the Navier-Stokes equations, but the usual no-slip condition at the boundary should be replaced by the slip condition [32]. Some authors [33,34] suggested the presence of a red blood cell slip at the vessel wall. Misra and Kar [35] developed a momentum integral method to investigate the problem of blood flow through a stenosed vessel by taking into consideration the slip velocity at the wall.

Modeling of hyperthermia-induced temperature distribution requires an accurate description of the mechanism of heat transfer. It is reported in [36] that blood flow is affected by the thermal response of living tissues. The rate of heat exchange between living tissues and the arterial network through blood flows depends on the geometry of the blood vessels and the flow variation of blood. Misra and Sinha [37] theoretically investigated the effect of magnetic field and thermal radiation on the flow and heat transfer in capillary blood vessels. They reported that velocity of blood can be controlled by suitably regulating the intensity of the external magnetic field. Craciunescu and Clegg [38] studied the effect of oscillatory flow on the resulting temperature distribution of blood and convective heat transfer in rigid vessels. The study of heat generation or absorption in moving fluids is also very much important in the dynamics of thermo-fluids. Heat generation can alter the temperature distribution in the fluid mass. Consequently, the particle deposition rate will be affected. Such studies bear the promise of important applications in the design of various biomedical appliances, as well as in nuclear reactors, electronic chips and semi-conductor wafers.

In this study, we are interested in the unsteady fluid flow and heat transfer of a fluid mass through a permeable vessel executing stretching motion under the action of an externally

applied magnetic field. The problem investigated here involves the effect of non-uniform heat source/sink. The thermal slip accompanied by velocity-slip at the capillary wall has been accounted for in the study. Because of the permeability of capillary blood vessel walls, consideration of the slip-velocity at the wall makes the study closer to the reality. The analysis of the model involves the solution of a set of nonlinear partial differential equations subject to the boundary conditions appropriate to the physical problem. In order to solve the boundary value problem, we have made an endeavor to develop a suitable numerical method that involves the use of finite differences, together with the method of discretization, where the matrix of unknown physical variables is diagonally dominant. The numerical results of various flow characteristics are presented graphically. The results indicate very clearly the threshold value of the magnitude of the magnetic field strength that should be applied to the human body. The study will be of profound interest to medical surgeons in regulating blood flow during surgery.

2. Mathematical formulation

Let us consider the unsteady two-dimensional incompressible laminar flow of blood through a permeable capillary under the action of a time dependent magnetic field $B(t)$, which acts in a direction transverse to that of the flow. It is assumed that the magnetic Reynolds number is much less than unity so that the induced magnetic field is negligible in comparison with applied magnetic field. The basic flow in the medium is entirely due to the buoyancy force caused by temperature difference between the wall and the inside medium. For the mathematical analysis that follows we use Cartesian coordinates (x, y), where x-axis is taken along the lower wall of the capillary, while y-axis is along in the transverse direction (see Fig. 1). The flow is driven by the stretching motion of the vessel wall, such that the velocity of the stretching sheet $U_w(x,t)$ can be written as

$$U_w(x,t) = \frac{ax}{1-ct}, \tag{1}$$

where a and c are both positive constants and $ct < 1$.

The expression (1) for the stretching velocity of the vessel emphasizes that the vessel, which is fixed at a point (taken as the origin of coordinates) is stretched by applying a force in the positive $x-$direction and the effective stretching rate $\frac{a}{1-ct}$ increase with time as $0 \leqslant c < 1$.

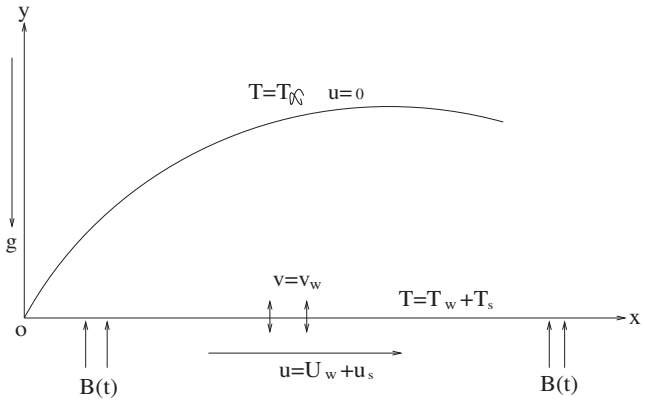

Figure 1 Physical sketch of the problem.

Here blood is considered as magnetohydrodynamic fluid properties independent of space and time at temperature T_∞. The walls of the artery are assumed to have non-uniform internal heat source/sink and at the lower wall temperature T_w is assumed to vary with the distance x from the slit at time t as

$$T_w = T_\infty + T_0 \frac{ax^2}{2v}(1-ct)^{-\frac{3}{2}}, \tag{2}$$

where T_0 is taken as a constant reference temperature and v is the kinematic coefficient of viscosity of blood.

The expression of the lower wall temperature $T_w(x,t)$ given by (2) represents a situation in which the lower wall temperature increases from T_∞ at the slit in proportional to x^2 and such that the amount of temperature enhancement along the sheet decreases with time.

The velocity-slip as well as the thermal slip will be taken into account.

The governing conservation equations of mass, momentum and energy at unsteady state can be expressed as

$$\frac{\partial u}{\partial x} + \frac{\partial v}{\partial y} = 0, \tag{3}$$

$$\frac{\partial u}{\partial t} + u\frac{\partial u}{\partial x} + v\frac{\partial u}{\partial y} = v\frac{\partial^2 u}{\partial y^2} - \frac{\sigma B^2(t)}{\rho}u - \frac{v}{k_1(t)}u \pm g\beta(T - T_\infty), \tag{4}$$

and

$$\frac{\partial T}{\partial t} + u\frac{\partial T}{\partial x} + v\frac{\partial T}{\partial y} = \frac{k}{\rho c_p}\frac{\partial^2 T}{\partial y^2} + \frac{1}{\rho c_p}q'''. \tag{5}$$

The definition of all the symbols involved in the equations is included in the Nomenclature.

The last term on the right hand side of the Eq. (4) represents the influence of thermal buoyancy force and the signs '$\pm$' indicate the flow assisting and flow opposing respectively.

The associated boundary conditions are

$$u = U_w + N\mu\frac{\partial u}{\partial y} = U_w + u_s, \quad v = V_w,$$
$$T = T_w + K\frac{\partial T}{\partial y} = T_w + T_s \qquad at\ y = 0 \tag{6}$$

and

$$u \to 0, \quad T \to T_\infty \qquad at \quad y \to \infty. \tag{7}$$

In Eq. (6), V_w represents the blood velocity at the vessel walls, given by

$$V_w = -\sqrt{\frac{va}{1-ct}}f(0), \tag{8}$$

where $V_w > 0$ in the case of injection and $V_w < 0$ in the case of suction.

In Eq. (4), $k_1(t) = k_2(1-ct)$ represents the time-dependent permeability parameter and in Eq. (6), $N = N_0(1-ct)^{\frac{1}{2}}$ denotes the velocity-slip factor, and $K = K_0(1-ct)^{\frac{1}{2}}$ stands for the thermal slip factor.

The time-dependence of the applied transverse magnetic field is considered to be of the form

$$B(t) = B_0(1-ct)^{-\frac{1}{2}}, \tag{9}$$

where B_0 is a constant, representing the magnetic field at $t = 0$.

The non-uniform heat generated or absorbed per unit volume is taken as

$$q''' = \frac{kU_w}{xv}\left[A^\star(T_w - T_\infty)e^{-\eta} + B^\star(T - T_\infty)\right], \tag{10}$$

where $A^\star$ and $B^\star$ are parameters of space-dependent and temperature-dependent heat generation/absorption (cf. [39]). $A^\star$ and $B^\star$ are both positive in the case of internal heat source and negative in the case of internal heat sink. Thus $q''' > 0$ in the case of heat generation; it is negative in the case of heat absorption.

2.1. Similarity solution for momentum and heat transfer equations

The governing Eqs. (4) and (5) admit a self-similar solution of the form

$$u = \frac{ax}{1-ct}f', \quad v = -\sqrt{\frac{va}{1-ct}}f, \quad \eta = \sqrt{\frac{U_w}{vx}}y \text{ and } \theta = \frac{T-T_\infty}{T_w - T_\infty}, \tag{11}$$

where f is the dimensionless stream function and η is the similarity variable.

It is evident that the non-dimensional variables satisfy the continuity Eq. (3).

Substituting these non-dimensional variables in Eq. (4), we obtain the following third-order nonlinear ordinary differential equation:

$$f''' + ff'' - f'^2 - S\left(f' + \frac{1}{2}\eta f''\right) - M^2 f' - \frac{1}{k_3}f' + \lambda\theta = 0, \tag{12}$$

where $M = \sqrt{\frac{\sigma}{\rho a}}B_0$ is the Hartmann number, $k_3 = \frac{ak_2}{v}$ is the permeability parameter, $S = \frac{c}{a}$ is the unsteadiness parameter, $\lambda = \frac{Gr_x}{Re_x^2}$ is the buoyancy parameter, $Gr_x = \frac{g\beta(T_w - T_\infty)x^3}{v}$ is the local Grashof number and $Re_x = \frac{U_w x}{v}$ is the local Reynolds number.

Here it is worthwhile to mention that $\lambda > 0$ in the flow assisting region, $\lambda < 0$ in the flow opposing region and $\lambda = 0$ represent the case when the buoyancy forces are absent.

Using the transformation (11), we can obtain the transformed energy equation from (5) as

$$\theta'' - Pr\left[\frac{1}{2}S(3\theta + \eta\theta') + 2f'\theta - \theta' f\right] + A^\star e^{-\eta} + B^\star\theta = 0, \tag{13}$$

in which $Pr = \frac{\mu c_p}{k}$ is the Prandtl number.

The boundary conditions (6) and (7) give rise to

$$f(0) = A, \quad f'(0) = 1 + S_f f''(0) \text{ and } \theta(0) = 1 + S_t\theta'(0) \tag{14}$$

and

$$f'(\eta) \to 0, \quad \theta(\eta) \to 0 \text{ as } \eta \to \infty. \tag{15}$$

In Eq. (13), $A < 0$ and $A > 0$ correspond to injection and suction respectively. The non-dimensional velocity-slip factor S_f and the non-dimensional thermal slip factor S_t are defined by

$$S_f = N_0\rho\sqrt{av} \text{ and } S_t = K_0\sqrt{\frac{b}{v}}.$$

2.2. Skin-fiction coefficient and local Nusselt number

The physical quantity of most interest in a problem such as the present one is the skin-friction coefficient (C_f), which is defined by the relation:

$$C_f = \frac{\tau_w}{\rho U_w^2/2}, \tag{16}$$

where the skin-friction on the flat plate τ_w is given by

$$\tau_w = -\mu\left(\frac{\partial u}{\partial y}\right)_{y=0}. \tag{17}$$

Using (11) and (17), we have from (16):

$$C_f = -2Re_x^{-\frac{1}{2}}f''(0). \tag{18}$$

Another important physical parameter of the current problem is the wall heat transfer coefficient (also called the local Nusselt number), which is defined as

$$Nu_x = \frac{q_w x}{k(T_w - T_\infty)}, \tag{19}$$

where the heat flux q_w on the stretching sheet is defined as

$$q_w = -k\left(\frac{\partial T}{\partial y}\right)_{y=0}. \tag{20}$$

Again using (11) and (20) in (19), we get

$$Nu_x = -Re_x^{\frac{1}{2}}\theta'(0). \tag{21}$$

3. Computational procedure

The system of coupled nonlinear ordinary differential Eqs. (12) and (13) along with the boundary conditions (14) and (15) has been solved numerically by employing a finite difference scheme. We use Newton's linearization method to linearize the discretized equations. The essential feature of this technique is that it is based on a finite difference scheme, which has better stability characteristics and is quite efficient. It is found to yield sufficiently accurate results. Application of the finite difference technique leads to a system, which is tridiagonal and therefore has speedy convergence. Moreover, it brings about economical memory space to store the coefficients. The computational work has been carried out by taking $\eta = 0.0125$. We have examined that further reduction in $\delta\eta$ does not produce any significant change. This ensures the stability of our numerical scheme. The finite difference scheme that we have developed is briefly described below.

Writing $f' = P$ in (12), we get

$$P'' + fP' - P^2 - S\left(P + \frac{1}{2}\eta P'\right) - M^2 P - \frac{1}{k_3}P + \lambda\theta = 0. \tag{22}$$

Also the boundary conditions (14) and (15) will now be of the form

$$f(0) = A, \qquad P(0) = 1 + S_f P'(0), \quad P(\infty) \to 0. \tag{23}$$

Using the central difference scheme for derivatives with respect to η, we can write

$$(G')_i = \frac{G_{i+1} - G_{i-1}}{2\delta\eta} + O((\delta\eta)^2) \tag{24}$$

and

$$(G'')_i = \frac{G_{i+1} - 2G_i + G_{i-1}}{(\delta\eta)^2} + O((\delta\eta)^2), \tag{25}$$

where G stands for P or θ; i is the grid index in η-direction with $\eta_i = i * \delta\eta$; $i = 0, 1, \ldots, m$; $\delta\eta$ is the increment along the η-axis.

Newton's linearization method can then be applied to linearize the discretized equations as described below.

When the values of the unknown functions at the n th iteration are known, the corresponding values of these variables at the next iteration are obtained by using the equation

$$G_i^{n+1} = G_i^n + (\Delta G_i)^n, \tag{26}$$

in which $(\Delta G_i)^n$ represents the error at the n th iteration, $i = 0, 1, 2, \ldots, n$. It is worthwhile to mention here that the error $(\Delta G_i)^n$ at the boundary is zero, because the values of G_i at the boundary are known. Using (26) in (22) and dropping the quadratic and higher order terms in $(\Delta G_i)^n$, we get a system of block tri-diagonal equations. To solve this tri-diagonal system of equations, we have used the "Tri-diagonal matrix algorithm", referred to as "Thomas algorithm".

In the process of determination of the distribution of the function $f(\eta)$, the accuracy can be defined as the difference between the calculated values of $f(\eta)$ at two successive operations, say $(n + 1)$th and nth.

In the present study, the error ϵ is equal to

$$\epsilon = |f^{n+1}(\eta) - f^n(\eta)|$$

and is estimated to be less than 10^{-6}.

4. Numerical estimates and related discussion

It is not possible to determine the exact solution of Eqs. (12) and (13) because of the nonlinearity of the momentum and thermal boundary layer equations. Thus we had to obtain the solution of the problem numerically. Appropriate similarity transformation has been adopted to transform the governing partial differential equations of flow and heat transfer into a system of nonlinear ordinary differential equations. The resulting boundary value problem is solved by developing a finite difference scheme with the help of Newton's linearization method described in the previous section.

For numerical solution it is necessary to assign some numerical values to the parameters involved in the problem under consideration. We find that the magnetic parameter M is approximately 4 when the system is under the influence of a strong magnetic field of strength $B_0 = 8$ T (Tesla), the blood density $\rho = 1050\ \mathrm{kg/m^3}$ and the electrical conductivity of blood, $\sigma = 0.8$ s/m.

Experimental reports reveal that like most other fluids, for human blood the viscosity μ, specific heat at constant pressure c_p and the thermal conductivity k are temperature-dependent. On the basis of their experimental studies, Valvano et al. [40] and Chato [9] reported the following data for human blood at a temperature $T = 310$ K:

$$\mu = 3.2 \times 10^3\ \mathrm{kg/ms}, c_p = 14.65\ \mathrm{J/kgK}, \text{and } k = 2.2 \times 10^{-3}\ \mathrm{J/msK}.$$

Using these data, we find that the value of the Prandtl number $Pr = \frac{\mu c_p}{k}$ for human blood is 21.

Numerical investigation was carried out with an aim to examine the variation of various physical variables for different cases, in the range: $0 \leqslant M \leqslant 5; S = 0, 0.3, 2.0, 5.0; A = 0, 0.5, 1.5, 2.0; \lambda = -15, -5, 5, 15; k_3 = 0.1, 0.2, 0.3, 0.4;$ $Pr = 18, 20, 21, 22, 23,$ $24, 27; S_f = 0.25; S_t = 0, 0.5, 1.0, 2.0; 0 \leqslant A^\star \leqslant 1$ and $B^\star = -0.5, -0.3, 0.05, 0.3, 0.5$. The computational work has been carried out by taking $\delta\eta = 0.0125$ with 401 grid points. The results computed have been presented graphically in Figs. 2–12. Fig. 13 establishes the validity of our results.

Distribution of non-dimensional axial velocity f' for different values of Hartmann number M, buoyancy parameter λ, velocity slip factor S_f, porosity permeability k_3 and unsteadiness parameter S is depicted in Figs. 2–6. The presence of a magnetic field in a direction normal to the flow in an electrically conducting fluid (e.g. blood) introduces a Lorentz force, which has a tendency to resist the flow. The resistive force tends to slow down the flow and hence the blood velocity decreases with the increase in the magnetic field strength, as observed from Fig. 2. This figure further indicates that blood velocity in the vessel is reduced with a increase in the distance from the lower wall. Fig. 3 gives an idea of the velocity

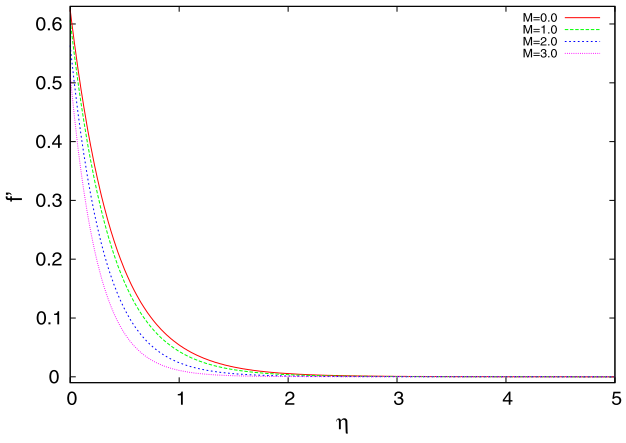

Figure 2 Velocity distribution for different values of M with $S = 0.3, S_f = 0.25, S_t = 1.0,\ k_3 = 0.2, A = 0.5, \lambda = 5.0, Pr = 21.0, A^\star = 0.05$ and $B^\star = 0.05$.

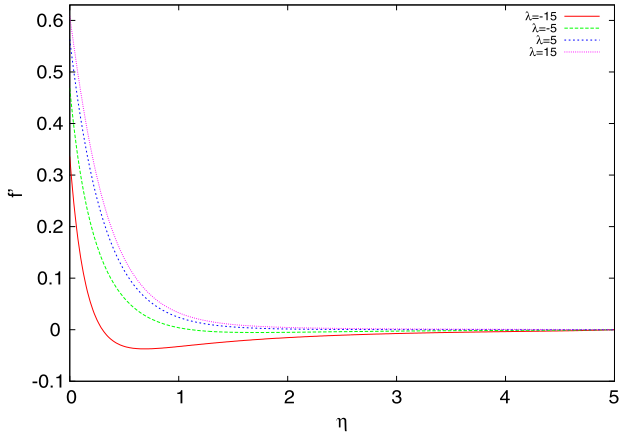

Figure 3 Velocity distribution for different values of λ, when $S = 0.3, S_f = 0.25, S_t = 1.0, k_3 = 0.2, A = 0.5, M = 2.0, Pr = 21.0, A^\star = 0.05$ and $B^\star = 0.05$.

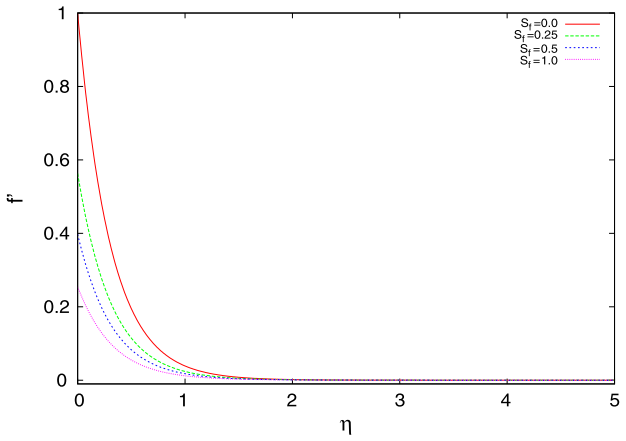

Figure 4 Velocity distribution for different values of S_f in a situation, where $S = 0.3, M = 2.0, S_t = 1.0, k_3 = 0.2, A = 0.5, \lambda = 5.0, Pr = 21.0, A^\star = 0.05$ and $B^\star = 0.05$.

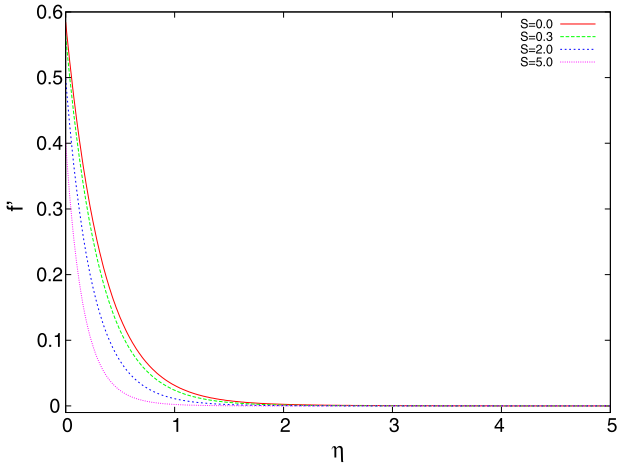

Figure 6 Velocity distribution for different values of S, when $M = 2.0, S_f = 0.25, S_t = 1.0, k_3 = 0.2, A = 0.5, \lambda = 5.0, Pr = 21.0, A^\star = 0.05$ and $B^\star = 0.05$.

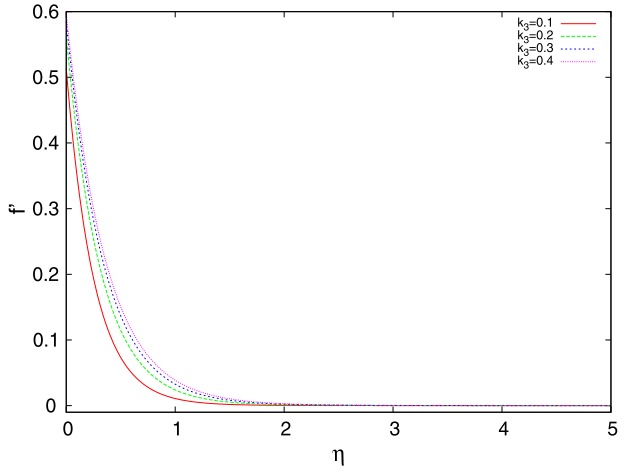

Figure 5 Velocity distribution for different values of k_3, when $S = 0.3, S_f = 0.25, S_t = 1.0, M = 2.0, A = 0.5, \lambda = 5.0, Pr = 21.0, A^\star = 0.05$ and $B^\star = 0.05$.

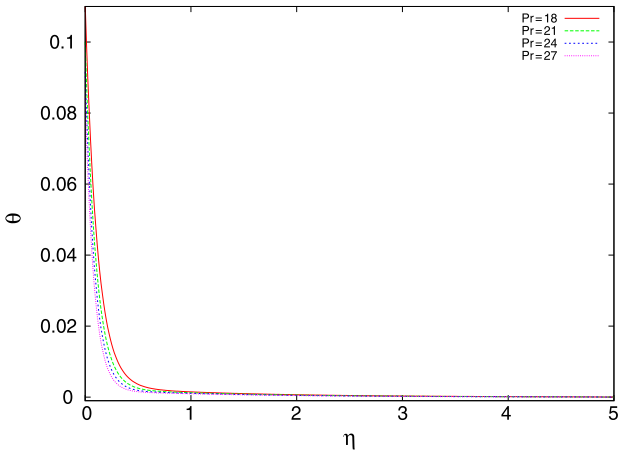

Figure 7 Temperature distribution for different values of Pr, in the situation when $M = 2.0, S_f = 0.25, S_t = 1.0, k_3 = 0.2, A = 0.5, \lambda = 5.0, S = 0.3, A^\star = 0.05$ and $B^\star = 0.05$.

distribution for different values of the buoyancy parameter λ. It is seen that blood velocity increases along the axis of the vessel, as the buoyancy parameter increases in the flow assisting region ($\lambda > 0$), while it decreases as the buoyancy parameter increases in the flow opposing region ($\lambda < 0$). Physically, $\lambda > 0$ means heating the fluid or cooling the stretching sheet, while $\lambda < 0$ implies cooling the fluid or heating the sheet, and $\lambda = 0$ corresponds to the free convection. This figure further shows that while cooling the walls of the vessel, the momentum boundary layer thickness increases, whereas when blood is cooled, there will occur a reduction in the boundary layer thickness. It is also seen that in the case of heating of the vessel walls, for large values of λ, velocity of blood vanishes at two different points. These points are the so-called points of inflexion. Fig. 4 describes the effects of the velocity-slip factor S_f on axial velocity in the case of cooling of the stretching wall. Clearly velocity in the axial direction reduces when the slip-velocity increases. In fact, the quantity $1 - f'(0)$ increases monotonically with the velocity-slip parameter S_f. So for large values of S_f, the frictional resistance between the blood and the vessel wall can be eliminated. Fig. 5 shows that blood velocity increases along the vessel-axis, with a rise in permeability. Moreover, for small permeability ($k_3 = 0.1$), the axial velocity reduces faster than when the permeability is higher ($k_3 = 0.2, 0.3, 0.4$). Fig. 6 gives the distribution of axial velocity for different values of the unsteadiness parameter S in the case of cooling of the vessel wall. It may be observed that the influence of S on axial velocity is similar when compared with Fig. 2.

Figs. 7–9 give some characteristic temperature profiles for different values of Prandtl number (Pr), heat source/sink parameter ($B^\star$) and temperature-jump parameter (S_t). Fig. 7 demonstrates the effect of Prandtl number (Pr) on temperature profile in the boundary layer. It may be observed that with the rise in Prandtl number, temperature of the boundary layer diminishes. This may be attributed to the fact that the thermal

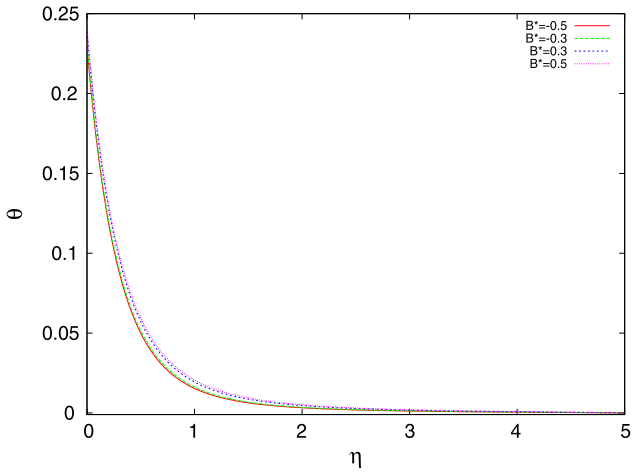

Figure 8 Temperature distribution for different values of $B^{\star}$, when $M = 2.0, S_f = 0.25, S_t = 1.0, k_3 = 0.2, A = 0.5, \lambda = 5.0, S = 0.3, A^{\star} = 0.05$ and $Pr = 21.0$.

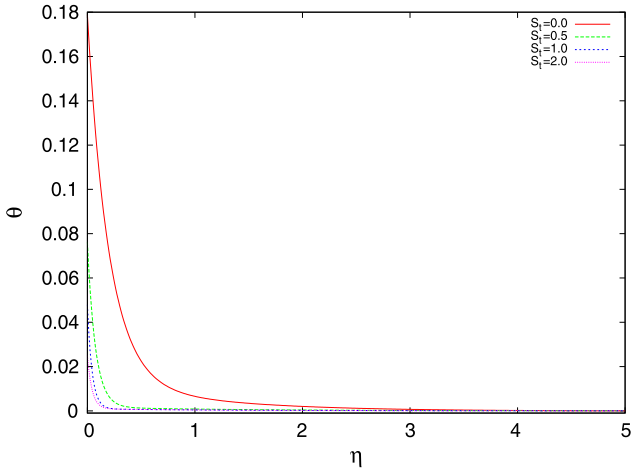

Figure 9 Temperature distribution for different values of S_t, with $M = 2.0, S_f = 0.25, Pr = 21.0, k_3 = 0.2, A = 0.5, \lambda = 5.0, S = 0.3, A^{\star} = 0.05$ and $B^{\star} = 0.05$.

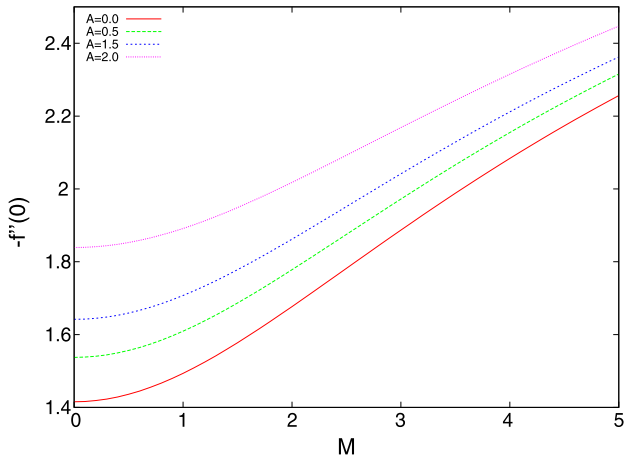

Figure 10 Variation of skin-friction with M for different values of suction parameter A, when $S_t = 1.0, S_f = 0.25, Pr = 21.0, k_3 = 0.2, \lambda = 5.0, S = 0.3, A^{\star} = 0.05$ and $B^{\star} = 0.05$.

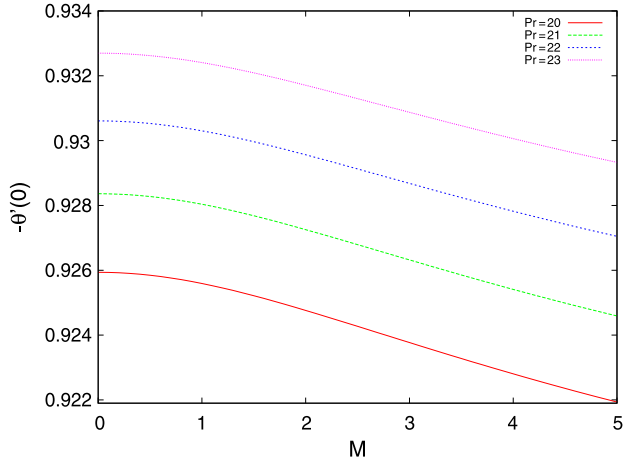

Figure 11 Variation of heat transfer coefficient with M for different values of Pr, in a situation when with $S_t = 1.0, S_f = 0.25, A = 0.5, k_3 = 0.2, \lambda = 5.0, S = 0.3, A^{\star} = 0.05$ and $B^{\star} = 0.05$.

boundary thickness decreases with a rise in Prandtl number. This figure further indicates that the temperature gradient at the surface increases with a rise in Prandtl number. This implies that an increase in Prandtl number is accompanied by an enhancement of the heat transfer rate at the wall of the blood vessel. When blood attains a higher Prandtl number, its thermal conductivity is lowered down and so its heat conduction capacity diminishes. Thereby the thermal boundary layer thickness gets reduced. Thus the heat transfer rate at the capillary wall is increased. The temperature profiles for different temperature-dependent parameters for heat source/sink are presented in Fig. 8. In the case of heat generation (when $B^{\star} > 0$), temperature of blood increases with increasing $B^{\star}$, while the reverse trend is observed in the case of heat absorption. Fig. 9 illustrates the changes that take place in the temperature distribution when the values of thermal slip factor (S_t) are changed. It is important to observe from this figure that the temperature reduces when thermal slip enhances (when $B^{\star} < 0$).

Fig. 10 shows the variation of skin-friction with the Hartmann number for different values of suction parameter A. From Eq. (18), it follows that the variation in $-f''(0)$ can represent the variation of the magnitude of the skin-friction coefficient. It is seen that skin-friction increases as the suction parameter A increases. From the same figure, it may also be observed that for any value of suction parameter, the skin-friction increases with increase in the value of the magnetic parameter M.

Figs. 11 and 12 present the variation of local Nusselt number for different values of Prandtl number (Pr) and unsteadiness parameter S respectively. Fig. 11 shows that local Nusselt number increases as the value of Prandtl number increases. It may be noted that the local Nusselt number diminishes as the magnetic field intensity is enhanced. Fig. 12

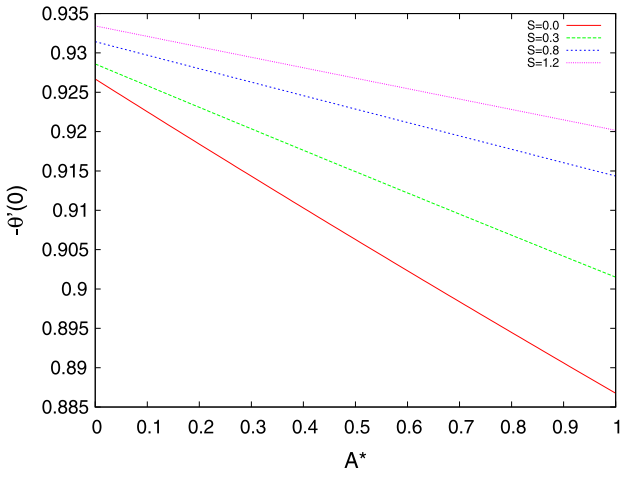

Figure 12 Variation of heat transfer coefficient with $A^{\star}$ for different values of the unsteadiness parameter S, when $M = 2.0, A = 0.5, S_t = 1.0, S_f = 0.25, Pr = 21.0, k_3 = 0.2, \lambda = 5.0$ and $B^{\star} = 0.05$.

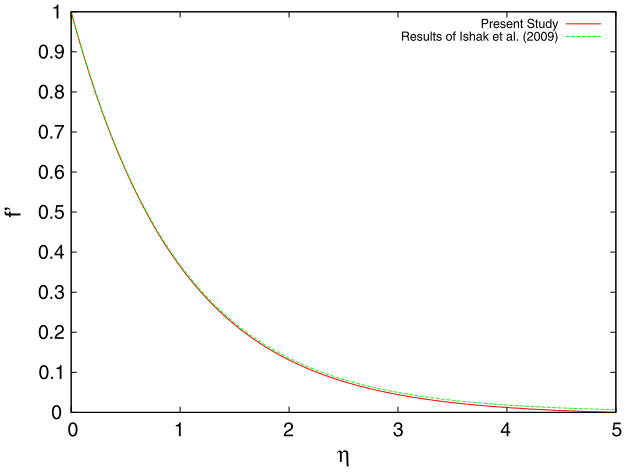

Figure 13 Velocity distribution function $f'(\eta)$: comparison of our results with those of Ishak et al. [41] for $M = S = S_f = \lambda = 0.0, A = 1.0$ and $k_3 = 100.0$.

indicates that the heat transfer rate is reduced as the space-dependent parameter for heat source $A^{\star}$ increases, while the heat transfer rate increases with the increase in the unsteadiness parameter S.

In Fig. 13, results of a previous investigation [41] have been presented along with the results of the present study. For the purpose of comparison, both the studies have been naturally brought to the same platform, by considering a vanishing value for the magnetic field parameter and also by disregarding the slip effects for the present study. For comparison, we also neglect the heat transfer effect, by setting $\lambda = 0$. Further, we assumed that the flow is steady, by taking the unsteadiness parameter $S = 0$ and we considered in our study a large value of the permeability parameter ($k_3 = 100.0$).

The analytical solution for $f(\eta)$ presented by Ishak et al. [41] is given by

$$f(\eta) = \zeta - \frac{1}{\zeta} e^{-\eta\zeta}, \text{ so that } f'(\eta) = e^{-\eta\zeta}$$

In their analysis, $f_0 = \zeta - \frac{1}{\zeta}$ (with $\zeta > 0$), and $0 < \zeta < 1$ and $\zeta > 1$ correspond to injection and suction respectively, while in the analysis of our model, S stands for the injection/suction parameter which is taken as 1.0.

One may observe from this figure that the results of the present study are in good agreement with those of the previous study [41].

5. Summary and conclusion

The problem of magneto-hydrodynamic flow of blood as well as the heat transfer in a permeable blood vessel, having a heat source/sink has been investigated here. The study is particularly applicable to a situation, where the lumen of the blood vessel has turned into a porous structure owing to a pathological condition. The vessel is considered to execute an unsteady stretching motion. The velocity-slip at wall and the thermal slip have been duly accounted for. The nonlinear governing equations are solved numerically by developing a suitable numerical technique with the help of Newton's linearization method.

The study bears the potential to explore some important information regarding the complex flow behavior of blood in situations where all the ten physical parameters $M, A, S, \lambda, k_3, S_f, S_t, Pr, A^{\star}$ and $B^{\star}$ play prominent roles in the hemodynamical flow and heat transfer in small blood vessels. The results presented here should be useful to clinicians, hematologists and biomedical engineers, because they serve as useful estimates, which are capable of throwing some light toward the understanding of genesis of pathological states, like arteriosclerosis as well as the mechanism of gaseous exchange that takes place within tissues and blood vessels. The following conclusions can be drawn on the basis of the numerical results reported in the preceding section.

(i) By the application of sufficiently strong magnetic field, blood velocity can be diminished. This is accompanied by a reduction in the velocity gradient at the vessel wall, whereby the local skin-friction can be reduced. The results presented should be of significant interest to surgeons who usually want to keep the blood flow rate at a desired level during the entire surgical procedure.

(ii) The buoyancy parameter has a dual effect on the axial velocity. The axial velocity increases in the flow assisting region ($\lambda > 0$) and decreases in the flow opposing region ($\lambda < 0$).

(iii) The velocity of blood along the axis of the capillary increases with a rise in permeability.

(iv) By increasing the Prandtl number Pr, it is possible to bring about a reduction in the thermal boundary layer thickness.

(v) With a rise in heat generation, thermal boundary layer thickness increases, but a reverse trend is observed in the case of heat absorption. This observation is of particular importance in the therapeutic procedure of electromagnetic hyperthermia used in the treatment of cancer, because the therapy involves rising the temperature of the cancerous tissues above 42 °C. An increase in

temperature brings down blood viscosity. While applying the procedure of hyperthermia, it is necessary to see that blood viscosity does not increase, because in that case there may arise various problems in respect of circulation of blood.

The present study can also be applied to deal with other problems that deal with different types of nonlinear variations of the velocity of the stretching surface subject to the action of a magnetic field, under the preview of the assumptions made here. Of course, the input values of the different physical parameters need to be changed as and when necessary.

Acknowledgment

One of the authors (A. Sinha) is grateful to the NBHM, DAE, Mumbai for the financial support of this investigation.

References

[1] Y.A. Cengel, A.J. Ghajar, Heat and Mass Transfer: Fundamentals and Applications, fourth ed., McGraw-Hill, 2010.
[2] J.C. Misra, A. Sinha, G.C. Shit, Flow of a biomagnetic viscoelastic fluid: application to estimation of blood flow in arteries during electromagnetic hyperthermia, a therapeutic procedure for cancer treatment, Appl. Math. Mech. – Engl. Ed. 31 (2010) 1405–1420.
[3] H. Barcroft, O.G. Edholm, The effect of temperature on blood flow and deep temperature in human forearm, J. Physiol. 102 (1943) 5–20.
[4] G.S. Barozzi, A.J. Dumas, Convective heat transfer coefficients in the circulation, J. Biomech. Eng. 113 (1991) 308–310.
[5] C.Y. Wang, Heat transfer to blood flow in a small tube, J. Biomech. Eng. 130 (2008) 024501, http://dx.doi.org/10.1115/1.2898722.
[6] H.H. Pennes, Analysis of tissue and arterial blood temperatures in the resting forearm, J. Appl. Physiol. 1 (1948) 93–122.
[7] A. Nakayama, F. Kuwahara, A general bioheat transfer model based on the theory of porous media, Int. J. Heat Mass Transfer 51 (2008) 3190–3199.
[8] M.C. Colios, M.D. Sherar, J.W. Hunt, Large blood vessel cooling in heated tissues: a numerical study, Phys. Med. Biol. 40 (1995) 477–494.
[9] J.C. Chato, Heat transfer to blood vessels, J. Biomech. Eng. 102 (1980) 110–118.
[10] K.N. Rai, S.K. Rai, Effect of metabolic heat generation and blood perfusion on the heat transfer in the tissues with a blood vessel, J. Biomech. Eng. 35 (1999) 75–79.
[11] A.L. Nilsson, Blood flow, temperature and heat loss of skin exposed to local radiative and convective cooling, J. Invest. Dermatol. 88 (1987) 586–593.
[12] Y. He, H. Liu, R. Himeno, M. Shirazaki, Numerical and experimental study on relationship between blood circulation and peripheral temperature, J. Mech. Med. Biol. 5 (2005) 39–53.
[13] Y. He, H. Liu, R. Himeno, A one-dimensional thermo-fluid model of blood circulation in the human upper limb, Int. J. Heat Mass Transfer 47 (2004) 2735–2745.
[14] L. Consiglieri, I. dos Sanotosh, D. Haemmerich, Theoretical analysis of the heat convection coefficient in large vessels and the significance for thermal ablative therapies, Phys. Med. Biol. 48 (2003) 4125–4134.
[15] J.W. Baish, Formulation of a statistical model of heat transfer in perfused tissues, J. Biomech. Eng. 116 (1994) 521–527.
[16] M.B. Ducharme, P. Tikuisis, Role of blood as heat source or sink in human limbs during local cooling and heating, J. Appl. Physiol. 76 (1994) 2084–2094.
[17] Q. He, D.E. Lemons, S. Weinbaum, L. Zhu, Experimental measurements of the temperature variation along artery-vein pairs from 200 to 1000 μm diameter in rat hind limb, J. Biomech. Eng. 124 (2002) 656–661.
[18] S. Srinivas, P.B.A. Reddy, B.S.R.V. Prasad, Effects of chemical reaction and thermal radiation on MHD flow over an inclined permeable stretching surface with non-uniform heat source/sink: An application to dynamics of blood flow, J. Mech. Med. Biol. 14 (2014) 1450067:1–1450067:24.
[19] V.A. Vardanyan, Effects of magnetic field on blood flow, Biofizika 18 (1973) 491–496.
[20] V.K. Sud, G.S. Sekhon, Blood flow through the human arterial system in the presence of a steady magnetic field, Physiol. Med. Biol. 34 (1989) 795–805.
[21] K. Haldar, S.N. Ghosh, Effect of a magnetic field on blood flow through an indented tube in the presence of erythrocytes, Ind. J. Pure Appl. Math. 25 (1994) 345–352.
[22] M.F. Barnothy, Biological Effects of Magnetic Fields, Plenum Press, New York, 1964, pp. 1964–1969.
[23] V.V. Kirkovskii, V.A. Mansurov, N.P. Mit'kovskaya, Y. Mukharskaya, Influence of a variable magnetic field on the rheological properties of blood in treatment of rheumatoid arthritis, J. Eng. Phys. Therm. Phys. 76 (2003) 708–714.
[24] S. Oka, T. Murata, A theoretical study of the flow of blood in a capillary with permeable wall, Jpn. J. Appl. Phys. 9 (1970) 345–352.
[25] N.K. Mariamma, S.N. Majhi, Flow of Newtonian fluid in a blood vessel with permeable wall – a theoretical model, Comp. Math. Appl. 40 (2000) 1419–1432.
[26] G.S. Beavers, D.D. Joseph, Boundary conditions at a naturally permeable wall, J. Fluid. Mech. 30 (1967) 197–207.
[27] P.G. Saffman, On the boundary condition at the surface of a porous medium, Stud. Appl. Math. 2 (1971) 93–101.
[28] J.C. Misra, G.C. Shit, Biomagnetic viscoelastic fluid flow over a stretching sheet, Appl. Math. Comput. 210 (2009) 350–361.
[29] J.C. Misra, G.C. Shit, Flow of a biomagnetic viscoelastic fluid in a channel with stretching walls, J. Appl. Mech. 76 (2009) 061006.
[30] J.C. Misra, G.C. Shit, H.J. Rath, Flow and heat transfer of an MHD viscoelastic fluid in a channel with stretching walls: some applications to hemodynamics, Comput. Fluids 37 (2008) 1–11.
[31] J.C. Misra, M.K. Patra, S.C. Misra, A non-Newtonian fluid model for blood flow through arteries under the stenotic conditions, J. Biomech. 26 (1993) 1129–1141.
[32] W.A. Ebart, E.M. Sparrow, Slip flow in rectangular and annular ducts, J. Basic Eng. 87 (1965) 1018–1024.
[33] P. Brunn, The velocity slip of polar fluids, Rheol. Acta 14 (1975) 1039–1054.
[34] Y. Nubar, Blood flow, slip and viscometry, J. Biophys. 11 (1971) 252–264.
[35] J.C. Misra, B.M. Kar, Momentum integral method for studying flow characteristics of blood through a stenosed vessel, Biorheology 26 (1989) 23–25.
[36] M.W. Dewhirst, T.V. Samulski, Hyperthemia in the Treatment for Cancer, Upjhon, Kalamazoo, MI, 1988.
[37] J.C. Misra, A. Sinha, Effect of thermal radiation on MHD flow of blood and heat transfer in a permeable capillary in stretching motion, Heat Mass Transfer 49 (2013) 617–628.
[38] O.I. Craciunescu, S.T. Clegg, Pulsatile blood flow effects on temperature distribution and heat transfer in rigid vessels, J. Biomech. Eng. 123 (2001) 500–505.
[39] R. Tsai, K.H. Huang, J.S. Huang, Flow and heat transfer over an unsteady stretching surface with non-uniform heat source, Int. Commun. Heat Mass Transfer 35 (2008) 1340–1343.

[40] J.W. Valvano, S. Nho, G.T. Anderson, Analysis of the Weinbaum-Jiji model of blood flow in the canine kidney cortex for self-heated thermistorsrom, J. Biomech. Eng. 116 (1994) 201–207.

[41] A. Ishak, R. Nazar, I. Pop, Heat transfer over an unsteady stretching permeable surface with prescribed wall temperature, Nonlinear Anal.: Real World Appl. 10 (2009) 2909–2913.